PUBLICATION

MUSTANG

A MUltiple Space and Time scale Approach for the quaNtification of deep saline formations for CO_2 storaGe

Project Number:227286

AUTHOR: *Víctor Vilarrasa*

TITLE: *Impact of CO_2 injection through horizontal and vertical wells on the caprock mechanical stability*

The research leading to these results has received funding from the European Community's Seventh Framework Programme [FP7/2007/2013) under grant agreement n° [227286]

Status	AUTHOR VERSION
Date	2014
Publisher	Science Direct
Reference	International Journal of Rock Mechanics and Mining Sciences, Vol. 66, pp. 151 - 159, 2014

Paper published in *International Journal of Rock Mechanics and Mining Sciences*, 66: 151-159

IMPACT OF CO_2 INJECTION THROUGH HORIZONTAL AND VERTICAL WELLS ON THE CAPROCK MECHANICAL STABILITY

Víctor Vilarrasa[1, 2]

[1] Lawrence Berkeley National Laboratory (LBNL), Berkeley, CA 94720, USA

[2] GHS, Institute of Environmental Assessment and Water Research (IDAEA), CSIC, Jordi Girona 18-26, 08034 Barcelona, Spain

ABSTRACT

Large amounts of carbon dioxide (CO_2) (of the order of several Gt/yr) will be injected in deep geological formations to reduce the emissions of greenhouse gases to the atmosphere, which will induce large overpressures that may put at risk the caprock mechanical stability. This overpressure may induce microseismic events if the rock yields. Yielding of the caprock could open up a leakage path for CO_2. Furthermore, if induced seismicity were felt by the local population, the public perception of geologic carbon storage projects could be damaged. Rock mechanical stability is strongly related to fluid pressure evolution, which is significantly different for vertical and horizontal wells. While CO_2 pressure builds up sharply at the beginning of injection but afterwards drops when injecting a constant CO_2 mass flow rate through a vertical well, a horizontal well leads to a continuous CO_2 pressure increase. Thus, for a vertical well, the less stable situation in the saline aquifer occurs at the beginning of injection. However, the changes induced in the effective stress field are small, so unstable conditions are unlikely both in a normal faulting and a reverse faulting stress regimes in extensive saline aquifers like the one considered in this study. By contrast, fluid pressure becomes larger than that of a vertical well for a common length of horizontal wells (around 2 km), which causes a significant increase in horizontal total stresses that improves the reservoir and caprock mechanical stability in a NF stress regime, but worsens it in a RF stress regime. Though in general the caprock mechanical stability is unlikely to be compromised, fluid pressure evolution should be always monitored and mitigation measures should be carried out if it deviates from its expected evolution.

Keywords: Geologic carbon storage, pressure buildup, hydro-mechanical coupling, induced microseismicity, Noordbergum effect.

1. INTRODUCTION

Geologic carbon storage (GCS) is a potential mitigation solution for reducing greenhouse gas emissions to the atmosphere. The large amounts of carbon dioxide (CO_2) (of the order of 8 Gt/yr by 2050 [1]) that will be injected in deep saline formations are likely to generate large overpressures that may jeopardize the caprock mechanical stability [2]. This overpressure may trigger induced microseismicity [3, 4, 5], which could lead to the open up of a leakage path for CO_2. Furthermore, induced seismic events could, according to numerical simulation [6, 7, 8], be felt by local population. If this occurred, the public perception of GCS would be damaged and CO_2 storage projects could eventually be stopped. In fact, public opposition has already led to the closure of the geothermal project Basel Deep Heat Mining Project in Switzerland [9]. Even though no felt seismic event related to CO_2 injection has been recorded to date [2], induced microseismic events have been measured by geophones placed at depth [10, 11]. As a result, coupled hydro-mechanical processes related to GCS are gaining importance and an increasing number of studies focus on this topic [12, 13, 14, 15, 16].

The hydro-mechanical response of the reservoir and caprock is strongly related to fluid pressure evolution, which is controlled by the orientation of the CO_2 injection well, i.e. vertical or horizontal well (Figure 1). CO_2 pressure evolution in a vertical well has been studied analytically in laterally extensive saline aquifers [17, 18] and in closed saline aquifers, i.e. surrounded by a low-permeability boundary [19, 20, 21]. The effect of a low-permeability boundary is an increase of overpressure in the whole saline aquifer, which may cause caprock mechanical instability. This increase in overpressure starts once the fluid pressure perturbation front reaches the low-permeability boundary. When injecting CO_2 at a constant mass flow rate through a vertical well, injection pressure

increases sharply at the beginning of injection both because the viscosity of the displaced brine is high and because the relative permeability to CO_2 is low before CO_2 establishes connected flow paths within the pore network and is able to flow readily. However, injection pressure slowly decreases once CO_2 fills the pores in the vicinity of the injection well and the capillary fringe is displaced away from the injection well because (i) the relative permeability to CO_2 increases around the well, (ii) the pressure drop across the capillary fringe is reduced (it is inversely proportional to the radius of the capillary fringe [14]) and (iii) the viscosity of CO_2 is much lower than that of the brine (around one order of magnitude). As a result, mechanical stability tends to improve with time. This fluid pressure evolution has been observed in the field in the Ketsin pilot test site, Germany [22], in a semianalytical solution [23] and in numerical simulations [14, 24, 25, 26]. By contrast, the injection of a constant CO_2 mass flow rate through a horizontal well induces a continuous increase of fluid pressure with time [25, 27]. This is mainly because relative permeability to CO_2 remains low between the injection well, which is usually placed at the bottom of the saline aquifer, and the top of the saline aquifer, where CO_2 accumulates and spreads laterally. Therefore, CO_2 cannot flow easily through well-connected paths, inducing a progressive buildup of injection pressure. This continuous increase in fluid pressure may yield failure conditions after several years of injection.

Given this significant difference between the fluid pressure evolution of vertical and horizontal wells, one may conjecture that CO_2 injection through vertical wells may be mechanically more favorable than through horizontal wells, at least for injection timescales of several decades. However, the stress field is usually modified as a result of fluid pressure changes [28]. Therefore, we perform fully coupled hydro-mechanical

simulations to analyze the suitability of CO_2 injection through horizontal and vertical wells and to determine whether the caprock mechanical stability could be damaged.

2. METHODS

2.1. Geometry

We consider an idealized horizontal saline aquifer overlaid and underlain by a low-permeability and high entry pressure formation (Figure 2). The aquifer has a thickness of 50 m and the thickness of the caprocks on top and below of the saline aquifer is 100 m. The top of the saline aquifer is placed at a depth of 1500 m. The model is completed by an upper aquifer that extends up to 500 m depth and by a basal aquifer that reaches a depth of 2500 m. We assume that the upper 500 m thick overburden has such a low shear stiffness that it does not need to be included in the model. The model extends laterally 100 km, so the outer boundary does not affect the hydro-mechanical behavior of the model. To represent the vertical and the horizontal wells, which have a radius of the casing of 0.15 m, we change the symmetry of the model. It is axisymmetric for the vertical well, while it is half of a 2D cross-section perpendicular to the horizontal well. The vertical well uniformly injects CO_2 along the whole thickness of the saline aquifer, while the horizontal well is placed at the bottom of the saline aquifer.

2.2. Rock properties

The hydro-mechanical properties of the rocks that form the model are listed in Table 1. The saline aquifer corresponds to a permeable sandstone and the caprocks to a shale [29]. The relative permeability curves follow a power law of saturation for both phases. This power law is cubic in the aquifers, while the power is 6 in the low-permeability rocks. The power is higher for the low-permeability formations (more concave curves)

because low-permability formations usually present higher multiphase interference effects than high-permeability rocks [30]. Retention curves follow the van Genuchten [31] model. The upper and basal aquifers have the same hydraulic properties, but the basal aquifer is stiffer because of its higher confining pressure. Apart from the base case scenario defined in Table 1, we analyze the effect of changing the caprock permeability and the stiffness of the saline aquifer.

2.3. Initial and boundary conditions

The initial conditions are hydrostatic pressure and constant temperature of 60 ºC (the mean temperature of the saline aquifer). We assume isothermal conditions during CO_2 injection. The initial stress field displays a relationship between horizontal and vertical effective stresses of either $\sigma'_{h_0} = 0.5\sigma'_{v_0}$ or $\sigma'_{h_0} = 2.0\sigma'_{v_0}$, where σ'_{h_0} is the initial horizontal effective stress, which is isotropic, $\sigma'_{v_0} = 0.013z$ MPa is the initial vertical effective stress and *z* is depth. The former case represents a normal faulting (NF) stress regime (the maximum principal stress is the vertical), which can be found in regions undergoing or that have undergone extension. The latter case represents a reverse faulting (RF) stress regime (the minimum principal stress is the vertical), which takes place in compressional regimes with constrained lateral deformation in the direction perpendicular to compression.

The hydraulic boundary conditions are constant hydrostatic pressure in the outer boundary and no flow in the other boundaries. The mechanical boundary conditions are a constant lithostatic stress on the upper boundary and no displacement perpendicular to the other boundaries (Figure 2).

The CO_2 is injected at a mass flow rate of 1 Mt/yr for 20 yr. The length of the horizontal well has been chosen to be equal to 2 km, which we deem is a common length of horizontal wells [2]. We also analyze the effect of varying the length of the horizontal well, or equivalently of changing the mass flow rate.

2.4. Rock stability analysis

Shear failure along pre-existing fractures is more likely than hydrofracturing of intact rock [2, 12, 29]. We assume that at any point there is a pre-existing fracture critically oriented for shear failure. To determine whether a pre-existing fracture is stable or not, we need to define a failure criterion. If the stress state falls below the failure envelope, the medium is stable and behaves elastically. However, if failure conditions are reached, the rock yields and a microseismic event is triggered. We adopt a Drucker-Prager failure criterion, which is defined in terms of the stress invariants as [32]

$$q = M\sigma'_m + \beta c\,, \tag{1}$$

where q is the deviatoric stress, σ'_m is the mean effective stress, c is cohesion and M and β are parameters that can be related to the friction angle, ϕ'. For a NF stress regime, these parameters are defined as

$$M = \frac{6\sin\phi'}{3-\sin\phi'}\,, \tag{2a}$$

$$\beta = \frac{6\cos\phi'}{3-\sin\phi'}, \tag{2b}$$

and for a RF stress regime, they are

$$M = \frac{6\sin\phi'}{3+\sin\phi'}\,, \tag{3a}$$

$$\beta = \frac{6\cos\phi'}{3+\sin\phi'}. \tag{3b}$$

The deviatoric stress is defined as

$$q = \sqrt{3J_2} = \frac{1}{\sqrt{2}}\sqrt{\left(\tau_{xx}-\tau_{yy}\right)^2+\left(\tau_{yy}-\tau_{zz}\right)^2+\left(\tau_{zz}-\tau_{xx}\right)^2+6\left(\tau_{xy}^2+\tau_{yz}^2+\tau_{zx}^2\right)} \quad (4)$$

where J_2 is the second invariant of the deviatoric stress tensor [33], τ_{ij} are the components of the stress tensor and $i, j = x, y, z$.

2.5. Numerical solution

The hydro-mechanical response of the rocks to CO_2 injection in a deep saline aquifer is simulated using the finite element numerical code CODE_BRIGHT [34, 35]. The mesh is made of structured quadrilateral elements. The mesh is finer close to the injection well in the saline aquifer and caprocks and becomes coarser further away. As a first step, a steady-state calculation is carried out to ensure consistent initial conditions in equilibrium for the pressure and stress fields.

3. RESULTS

Since fluid pressure evolution is significantly different when injecting CO_2 through a vertical well than through a horizontal well, the induced changes in the effective stress field differ as well. This is reflected in a plot that shows the deviatoric stress versus the mean effective stress ($q - \sigma'_m$) trajectories (Figures 3 and 4). When injecting a constant mass flow rate of CO_2 through a vertical well, the sharp increase in fluid pressure at the beginning of injection produces, in the saline aquifer, a rapid decrease in the mean effective stress, while the deviatoric stress remains nearly constant (Figure 3a and 4a). Thus, the stress state approaches failure conditions at the beginning of injection. However, once CO_2 pressure drops, the mean effective stress increases, leading to a safer situation. Additionally, horizontal total stresses increase as a response to fluid

pressure buildup [2, 14, 28, 36]. This causes the deviatoric stress to decrease in a NF stress regime (because the horizontal stress is the minimum and since it increases, the Mohr circle becomes smaller) and to increase in a RF stress regime (because the horizontal stress is the maximum and since it increases, the Mohr circle becomes bigger). Fluid pressure evolution in the caprock is somewhat different because of mechanical effects that lead to a pressure drop at the beginning of injection rather than an increase, which is known as the Noordbergum effect [29, 37]. This leads to an improvement of the caprock mechanical stability at the beginning of injection that is followed by a small decrease in stability once overpressure propagates across the low-permeability caprock, which can last several days or weeks (Figure 3b and 4b). This decrease in caprock stability is more pronounced in a RF stress regime than in a NF stress regime because in a RF stress regime the deviatoric stress increases as the horizontal total stresses increase.

On the other hand, CO_2 pressure builds up progressively when injecting CO_2 through a horizontal well. This results in a simultaneous reduction in the mean effective stress and deviatoric stress that yields a $q-\sigma'_m$ trajectory that is almost parallel to the failure envelope in a NF stress regime (Figure 3a). Similarly, the trajectory in the caprock is quite parallel to the failure envelope (except for some abrupt changes in the trajectory direction that are due to CO_2 breaking through into the caprock and will be explained in detail later). So despite the continuous CO_2 pressure buildup, failure conditions are unlikely to occur in this particular scenario (Figure 3b). However, in a RF stress regime the deviatoric stress in the saline aquifer increases rather than decreases as fluid pressure builds up (Figure 4a). This trend also occurs in the caprock (Figure 4b), which presents some abrupt changes in the trajectory direction that are due to CO_2 breaking through into the caprock.

These results may be surprising because, while it is clear that the mean effective stress decreases when fluid pressure increases, it may not be obvious why the deviatoric stress should change. Figures 5 and 6, which display the overpressure, the deviatoric and the mean effective stress evolution in the reservoir, show that the mean effective stress decreases as CO_2 pressure increases, but the magnitude of the mean effective stress decrease is smaller than that of overpressure. This is because horizontal total stresses increase when injecting a fluid due to lateral confinement [14, 36] and the magnitude of the increase in the horizontal total stresses is proportional to overpressure [2, 38]. Figures 5 and 6 also show the mobilized friction angle, ϕ'_{mob}, calculated assuming cohesionless fractures and using the relationship between the friction angle and the ratio of deviatoric to mean effective stress given by Eq. (2a) and (3a) for a NF and a RF stress regime, respectively. The most critical situation in the saline aquifer occurs at the beginning of CO_2 injection when it is performed through a vertical well (Figures 5a and 6a). The mobilized friction angle decreases after the initial peak in a NF stress regime because the deviatoric stress decreases, while it remains nearly constant in a RF stress regime because the deviatoric stress increases slightly. Similarly, CO_2 injection through a horizontal well induces a decrease of the mobilized friction angle in a NF stress regime, but without the initial peak that occurs in a vertical well (Figure 5b). This is because both the mean effective stress and the deviatoric stress are reduced since the beginning of injection. Note that the overpressure induced by this horizontal well, of 2 km in length, is much higher than that induced by the vertical well. Therefore, the increase in horizontal total stresses is larger, which is reflected in the RF stress regime considered in this study, which mobilizes a friction angle of almost 35º after 20 yr of injection (Figure 6b).

Figures 7 and 8 show the overpressure, the deviatoric and the mean effective stress evolution in a point of the caprock that is placed next to the well casing and 5 m above the saline aquifer. This point is representative of the lower region of the caprock, which is the most critical because of its proximity to the saline aquifer. When injecting through a vertical well (Figures 7a and 8a), fluid pressure drops at the beginning of injection (for a few days) because of the deformation induced by injection, which produces an expansion of the pore volume within the caprock. This leads to an improvement of the caprock mechanical stability at the beginning of injection, which is followed by a worsening as fluid pressure perturbation propagates through the low-permeability caprock. Nevertheless, the changes are small in the scenarios considered in this study, so the caprock mechanical stability is unlikely to be compromised unless the rock is critically stressed. For a horizontal well (Figure 7b and 8b), the caprock mechanical stability presents some abrupt changes in stability, which are related to CO_2 breaking through into the caprock. CO_2 penetrates into the caprock in this particular case because of the high overpressure, which leads to a capillary pressure higher than the caprock entry pressure. Initially, the induced overpressure in the saline aquifer propagates into the lower part of the caprock, but with a lower magnitude. Therefore, horizontal stresses increase in the caprock, causing an improvement in caprock stability in a NF stress regime (because the deviatoric stress decreases) and a worsening in a RF stress regime (because the deviatoric stress increases). When CO_2 first penetrates into the caprock (after 6 yr of injection), it causes an increase of the horizontal total stresses, which tightens the lower part of the caprock, where CO_2 has not arrived yet. This specially affects a caprock in a NF stress regime, improving the caprock mechanical stability (Figure 7b). However, this effect is much smaller in a RF stress regime, because the confining stress is already large (Figure 8b). But once CO_2 reaches the observation

point (after 12 yr), fluid pressure increases sharply, which produces a decrease of effective stresses. Thus, stability is worsened significantly, which could contribute to an enhancement of CO_2 flux through the caprock if it were to yield.

Figure 9 illustrates the mobilized friction angle as a function of depth at the beginning of injection (1 day) and after a long time of injection (20 years) for a vertical and a horizontal well in a NF and a RF stress regimes. The mobilized friction angle increases in the whole reservoir at the beginning of injection when CO_2 is injected through a vertical well for both a NF and a RF stress regimes. However, it decreases in a NF stress regime for long injection times due to the CO_2 pressure drop and the increase of horizontal total stresses, which reduces the deviatoric stress (Figure 9a). The most critical point coincides with the top of the saline aquifer, because it is the point with the lowest confining pressure affected by the high overpressure that occurs in the saline aquifer (overpressure dissipates rapidly in the caprock because of its low-permeability). In a RF stress regime (Figure 9b) the mobilized friction angle remains nearly constant in the saline aquifer and increases gradually in the caprock, but always presenting lower values than in the reservoir. On the other hand, the mechanical stability of the saline aquifer and caprock is almost unaffected at the beginning of injection when injecting through a horizontal well. However, the progressive pressure buildup and the subsequent increase in horizontal total stresses produce a decrease of the mobilized friction angle within the saline aquifer in a NF stress regime, and an increase in a RF stress regime. The region of the caprock in which CO_2 has penetrated (the lower 25 m of the caprock) can be distinguished because of the change in the mobilized friction angle. In a NF stress regime (Figure 9a) the changes are more pronounced because of the lower confinement. The CO_2 front coincides with the maximum mobilized friction angle caused by the sudden decrease in effective stresses that the arrival of CO_2

produces. There is a local minimum of the mobilized friction angle above the CO_2 desaturation front because the horizontal total stresses increase above the CO_2 front. This is the same sequence as the one shown in Figure 7b, but here in space rather than in time. In a RF stress regime (Figure 9a) the region of the caprock that contains CO_2 presents a higher mobilized friction angle because of the reduction in the mean effective stress.

We also analyze if changing some parameters of the model alter the hydro-mechanical response of the system to CO_2 injection. First, we consider the effect of the caprock being two orders of magnitude more permeable. A more permeable caprock permits a more rapid propagation of fluid pressure perturbation, thus reducing the effective stresses in the caprock, which could bring the stress state closer to failure conditions. Second, we reduce the stiffness of the aquifer to obtain an aquifer that is softer than the caprock (by a factor of 2). In this situation, more stress can be transferred from the aquifer to the caprock [11]. Finally, we study the effect of varying the mass flow rate and the length of the horizontal well, which has a direct effect on the induced overpressure.

Table 2 collects the maximum mobilized friction angle for the base case (recall Table 1), for a model with a more permeable caprock (two orders of magnitude), for a model with an aquifer that is softer than the caprock (by a factor of 2), for a higher mass flow rate (double) and a longer horizontal well that induces an overpressure similar to that of the vertical well (for a mass flow rate of 1 Mt/yr). The maximum mobilized friction angle in the saline aquifer occurs at the beginning of injection when injecting through a vertical well both in a NF and in a RF stress regimes. However, for a horizontal well it occurs at the end of injection (20 years in our simulations), except when a high overpressure is induced in a NF stress regime. In the latter case, the horizontal total

stresses increase significantly and cause such a decrease in the deviatoric stress that the rock mechanical stability improves with time. The change of these parameters has a similar effect on the reservoir for both types of well. A higher mass flow rate induces a larger overpressure, which causes a higher reduction in the mean effective stress that leads to a higher maximum mobilized friction angle. A softer aquifer has little effect on the reservoir stability. Furthermore, the overpressure is smaller in the presence of a caprock with a higher permeability because a larger amount of brine can flow through it, resulting in a lower mobilized friction angle in the saline aquifer. The later is not true for a horizontal well in a NF stress regime, because for this case the decrease is the deviatoric stress due to the increase in the horizontal total stresses is smaller than the decrease in the mean effective stress due to the progressive pressure buildup. This leads to a slight increase of the mobilized friction angle with time, but at such a small rate that it seems unlikely that the aquifer mechanical stability would be jeopardized, even though injection last for several decades. By contrast, the reservoir may yield for horizontal wells in a RF stress regime when overpressure builds up significantly because the increase in the horizontal total stresses leads to a continuous increase of the deviatoric stress.

In the caprock, the injection mass flow rate has little effect on the caprock mechanical stability in a NF stress regime, but in a RF stress regime the caprock stability decreases as overpressure in the caprock increases. A higher permeability of the caprock increases its maximum mobilized friction angle in a NF stress regime because overpressure can propagate more easily inside the caprock, reducing the effective stresses. But, in a RF stress regime the mobilized friction angle becomes smaller because the lower overpressure that is induced in the reservoir leads to smaller changes in the stress field. A softer aquifer leads to a higher mobilized friction angle in the caprock in a NF stress

regime, but a lower one in a RF stress regime because the changes in horizontal total stresses are smaller in a softer aquifer [2, 38] and therefore the changes in the caprock are also smaller. Finally, a horizontal well which length is such that the induced overpressure is similar to that induced by a vertical well (for a mass flow rate of 1 Mt/yr), mobilizes friction angles that are in the same order of magnitude than the ones that mobilizes a vertical well. However, such a length is 8 km, which is significantly longer than conventional horizontal wells.

The sensitivity analysis also includes the quantification of CO_2 flux through the caprock. Figure 10 displays the vertical CO_2 flux across a horizontal section of the caprock that is placed 5 m above the saline aquifer after 20 yr of injection. The highest vertical CO_2 flux in the lower part of the caprock corresponds to a horizontal well of 2 km in length, which induces a large overpressure. The flux close to the injection well is very similar regardless of the caprock permeability. However, far away from the injection well, the CO_2 flux decreases for a caprock permeability of 10^{-18} m^2, but remains nearly constant within the whole area of the CO_2 plume for a more permeable caprock (by two orders of magnitude). Thus, what prevents CO_2 from entering into the caprock is the capillary entry pressure rather than the caprock permeability. However, once CO_2 enters into the caprock, a more permeable caprock will allow a higher CO_2 flux through it, especially far away from the injection well, where pressure gradients are smaller. The average vertical CO_2 flux for the more permeable caprock is around 10^{-11} m/s and occurs for an area of $2 \cdot 2000 \cdot 4000$ m^2, which yields a flow rate of $1.6 \cdot 10^{-4}$ m^3/s. For the pressure and temperature conditions of this injection scenario, CO_2 density is around 660 kg/m^3. Therefore, the mass flow rate that flows through the lower part of the caprock, and therefore is escaping from the saline aquifer, is of 0.1 kg/s, which is a 0.3 % of the injected CO_2 mass flow rate. By contrast, the vertical CO_2 flux is almost

negligible for the vertical well, which induces a lower overpressure. We show for comparison the vertical CO_2 flux that corresponds to a horizontal well of 8 km in length, which induces an overpressure similar to that of the vertical well. The vertical CO_2 flux is larger than for the vertical well, but still can be considered as negligible.

4. DISCUSSION

The conjecture that the rock mechanical stability would be more favorable for CO_2 injection through vertical than horizontal wells for long injection times (decades) is not necessarily valid. This is because even though fluid pressure increases continuously when injecting through a horizontal well, horizontal total stresses also increase, leading to a reduction of the deviatoric stress for a NF stress regime. However, this increase in the horizontal total stresses enlarges the deviatoric stress in a RF stress regime, leading to unstable conditions both in the saline aquifer and the caprock. Therefore, microseismic events are likely to occur, which could open up leakage paths. On the other hand, the most critical situation in the saline aquifer occurs at the beginning of injection through a vertical well, coinciding with the peak in overpressure. To minimize the risk of inducing microseismicity, CO_2 injection rate can be progressively increased at the beginning, so that fluid pressure builds up more gradually. However, induced microseismic events are not necessarily negative if they are triggered within the saline aquifer because microseismicity is related to shear slip, which increases permeability of rough fractures, especially in the direction perpendicular to shear [39, 40, 41]. Therefore, injectivity would be enhanced and a lower overpressure would be necessary for injecting the same amount of CO_2.

From the sensitivity analysis, induced microseismicity in the caprock is more likely to occur in the presence of caprocks with a relatively high permeability, because fluid

pressure can propagate more easily through them. In fact, Vilarrasa et al. [14] modeled a case in which a caprock with a relatively high permeability yielded as a result of CO_2 injection at a high mass flow rate (3.6 Mt/yr). Caprocks with a relatively high permeability are not rare in nature, because even though the matrix permeability can be very low, the presence of fractures can contribute to an increase of permeability of two to three orders of magnitude at the kilometric scale [42], which is the scale of interest in geologic carbon storage.

The length of the horizontal well considered in this study is 2 km, which is within the range of most horizontal wells. The induced overpressure is higher (by a factor of 4 in this scenario) than that of a vertical well. Thus, a higher overpressure than for the vertical well will be necessary to inject the same amount of CO_2. This leads to a higher compression cost for horizontal wells. Therefore, the length of a horizontal well should be decided according to a drilling cost to efficiency trade-off. For instance, to obtain an overpressure in the range of that induced by the vertical well, the length of the horizontal well should be of 8 km for this particular case. Though such a well is relatively long, it is shorter than the longest horizontal well, which is almost 11 km long [43], so its drilling is technically feasible. In the presence of thick aquifers, vertical wells seem to be more effective because a few million tonnes of CO_2 can be injected while maintaining an overpressure below the maximum sustainable injection pressure. Furthermore, vertical wells provide higher storage efficiency than horizontal wells when the aquifer permeability is strongly anisotropic [44]. Nevertheless, to maximize the use of pore space, it should be ensured that CO_2 enters the saline aquifer along the whole thickness of the aquifer. Under some circumstances that result in gravity forces dominating viscous forces around the injection well (generally in high permeability aquifers), CO_2 may be only injected through the top portion of the saline aquifer [23]. In

these cases, a horizontal well placed at the bottom of the aquifer would lead to a higher spreading of the CO_2 plume, increasing dissolution and capillary trapping. Therefore, horizontal wells may be more effective in thin saline aquifers, like in the case of In Salah, Algeria [2] or placed at the bottom of aquifers in which gravity forces dominate, like in the case of Sleipner, Norway [45].

The overpressure induced by the horizontal well considered in this study is similar to that of In Salah, Algeria [46], i.e. 10 MPa. Though the mechanisms are different in each case, such overpressure is high enough for CO_2 to penetrate into the caprock. In this study CO_2 penetrates into the caprock because the capillary pressure exceeds the caprock entry pressure, while in In Salah the overpressure opens up a existing set of fractures that permit the upwards flow of CO_2 [47]. However, in both cases CO_2 remains in the lower part of the caprock, so CO_2 does not leak to upper formations which could potentially contain freshwater.

Thermal effects also affect the rock mechanical stability [38, 48, 49], but they have not been studied here. CO_2 will usually reach the saline aquifer at a lower temperature than that of the reservoir because it does not equilibrate with the geothermal gradient on its way down to the reservoir [50]. Therefore, effective stresses will be reduced in the saline aquifer due to thermal contraction of the rock, potentially causing the stress state to approach failure conditions. However, the caprock mechanical stability improves for a NF stress regime because the stress drop in the reservoir causes the horizontal total stresses to increase in the caprock [38]. But in a RF stress regime the caprock stability remains similar to that of an isothermal injection [38]. Therefore, horizontal wells that would induce large overpressures in a RF stress regime are not recommended because the caprock integrity is likely to be jeopardized, which could trigger induced microseismic events and CO_2 may leak through the caprock.

Here, we have considered a saline aquifer of extensive lateral dimensions. However, heterogeneity, such as faults, may exist relatively close to the injection well. If a fault behaves as a flow barrier, overpressure will increase [14, 19, 20], which eventually could trigger induced seismicity [8]. Undetected flow barriers can pose a risk to rock mechanical stability if fluid pressure increases significantly. Therefore, monitoring injection pressure evolution is crucial to guarantee that induced seismicity that could be felt by local population will not be triggered and that no leakage path is created. Deviations from the expected fluid pressure evolution should be analyzed and mitigation measures should be carried out if overpressure increases unexpectedly.

5. CONCLUSIONS

CO_2 pressure evolution is significantly different when injecting a constant CO_2 mass flow rate through a vertical or a horizontal well. Fluid pressure near the injection well increases sharply at the beginning of injection (for a few days) through a vertical well, but afterwards it drops slightly. Therefore, the rock mechanical stability is reduced in the saline aquifer at the beginning of injection, but it improves after the initial peak in fluid pressure. Nevertheless, the induced changes are small in the cases considered in this study. By contrast, fluid pressure continuously builds up when injecting through a horizontal well and for a common length of horizontal wells (around 2 km) the induced overpressure is larger than that of a vertical well. Not only does overpressure produce a gradual reduction in the mean effective stress, but also an increase of the horizontal total stresses because of the lateral confinement. When overpressure is significantly high (of the order of 10 MPa), the increase of horizontal total stresses leads to a more stable situation in the NF stress regime considered in this study (the deviatoric stress decreases), but could lead to unstable conditions in a RF stress regime (the deviatoric

stress increases). This high overpressure gives rise to a capillary pressure that exceeds the caprock entry pressure, so CO_2 penetrates through the lower portion of the caprock. However, overpressure becomes comparable of that induced by a vertical well in the presence of a caprock with a relatively high permeability or a longer injection well. In these cases, neither the reservoir nor the caprock mechanical stability is likely to be compromised because the effective stress changes induce relatively small changes in the mobilized friction angle. Thus, CO_2 injection at a constant mass flow rate through a vertical well is unlikely to yield unstable conditions both in NF and RF stress regimes in extensive saline aquifers like the one considered in this study. However, when injecting through a horizontal well the increase in horizontal total stresses improves the reservoir and caprock mechanical stability in a NF stress regime, but worsens it in a RF stress regime when a high overpressure is induced. These changes in the stress field highlight the importance of solving coupled hydro-mechanical simulations to assess the rock mechanical stability of geologic carbon storage projects.

ACKNOWLEDGEMENTS

This work has been funded by Fundación Ciudad de la Energía (Spanish Government) (www.ciuden.es) through the project ALM/09/018 and by the European Union through the "European Energy Programme for Recovery" and the Compostilla OXYCFB300 project. We also want to acknowledge the financial support received from the 'MUSTANG' (www.co2mustang.eu) and 'PANACEA' (www.panacea-co2.org) projects (from the European Community's Seventh Framework Programme FP7/2007-2013 under grant agreements nº 227286 and nº 282900, respectively).

REFERENCES

[1] International Energy Agency. Energy Technology Perspective. Scenarios and Strategies to 2050. 2010.

[2] Rutqvist J. The geomechanics of CO_2 storage in deep sedimentary formations. Geotechn. Geol. Eng. 2012; 30:525–51.

[3] Hsieh PA, Bredehoeft JD. A reservoir analysis of the Denver earthquakes: A case of induced seismicity. J. Geophys. Res. 1981; 86(B2):903-20.

[4] Soltanzadeh H, Hawkes CD. Assessing fault reactivation tendency within and surrounding porous reservoirs during fluid production or injection. Int. J. Rock Mech. Min. Sci. 2009; 46:1-7.

[5] Evans KF, Zappone A, Kraft T, Deichmann N, Moia F. A survey of the induced seismic responses to fluid injection in geothermal and CO_2 reservoirs in Europe. Geothermics 2012; 41:30-54.

[6] Cappa F, Rutqvist J. Impact of CO_2 geological sequestration on the nucleation of earthquakes. Geophys. Res. Lett. 2011; 38, L17313, doi:10.1029/2011GL048487.

[7] Cappa F, Rutqvist J. Seismic rupture and ground accelerations induced by CO_2 injection in the shallow crust. Geophys. J. Int. 2012; 190:1784-89.

[8] Mazzoldi A, Rinaldi AP, Borgia A, Rutqvist J. Induced seismicity within geologic carbon sequestration projects: Maximum earthquake magnitude and leakage potential. Int. J. Greenh. Gas Control 2012; 10:434–42.

[9] Häring MO, Schanz U, Ladner F, Dyer BC. Characterization of the Basel 1 enhanced geothermal system. Geothermics 2008; 37:469–95.

[10] Bohnhoff M, Zoback MD, Chiaramonte L, Gerst JL, Gupta N. Seismic detection of CO_2 leakage along monitoring wellbores. Int. J. Greenh. Gas Control 2010; 4 (4):687–97.

[11] Verdon JP, Kendall J-M, White DJ, Angus DA. Linking microseismic event observations with geomechanical models to minimise the risks of storing CO_2 in geological formations. Earth and Planetary Sci. Lett. 2011; 305:143-52.

[12] Rutqvist J, Birkholzer JT, Tsang C-F. Coupled reservoir-geomechanical analysis of the potential for tensile and shear failure associated with CO_2 injection in multilayered reservoir-caprock systems. Int. J. Rock Mech. Min. Sci. 2008; 45:132-43.

[13] Ferronato M, Gambolati G, Janna C, Teatini P. Geomechanical issues of anthropogenic CO_2 sequestration in exploited gas fields. Energy Convers. Manage. 2010; 51:1918–28.

[14] Vilarrasa V, Bolster D, Olivella S, Carrera J. Coupled hydromechanical modeling of CO_2 sequestration in deep saline aquifers. Int. J. Greenh. Gas Control 2010; 4 (6):910–19.

[15] Goerke U-J, Park C-H, Wang W, Singh AK, Kolditz O. Numerical simulation of multiphase hydromechanical processes induced by CO_2 injection into deep saline aquifers. Oil & Gas Sci. Tech. 2011; 66:105-18.

[16] Alonso J, Navarro V, Calvo B, Asensio L. Hydro-mechanical analysis of CO_2 storage in porous rocks using a critical state model. Int. J. Rock Mech. Min. Sci. 2012; 54:19-26.

[17] Mathias SA, Hardisty PE, Trudell MR, Zimmerman RW. Approximate solutions for pressure buildup during CO_2 injection in brine aquifers. Transp. Porous Media 2009; 79:269–84.

[18] Vilarrasa V, Bolster D, Dentz M, Olivella S, Carrera J. Effects of CO_2 Compressibility on CO_2 Storage in Deep Saline Aquifers. Transp. Porous Media 2010; 85:619–39.

[19] Zhou Q, Birkholzer J, Tsang C-F, Rutqvist J. A method for quick assessment of CO_2 storage capacity in closed and semi-closed saline formations. Int. J. Greenh. Gas Control 2008; 2:626–39.

[20] Mathias SA, Gonzalez Martinez de Miguel GJ, Thatcher KE, Zimmerman RW. Pressure buildup during CO_2 injection into a closed brine aquifer. Transp. Porous Media 2011; 89:383–97.

[21] Mathias SA, Gluyas JG, Gonzalez Martinez de Miguel GJ, Hosseini SA. Role of partial miscibility on pressure buildup due to constan trate injection of CO_2 into closed and open brine aquifers. Water Res. Res. 2011; 47, W12525, doi:10.1029/2011WR011051.

[22] Henninges J, Liebscher A, Bannach A, Brandt W, Hurter S, Köhler S, Möller F and CO_2SINK Group. P-T-ρ and two-phase fluid conditions with inverted density profile in observation wells at the CO_2 storage site at Ketsin (Germany). Energy Procedia 2011; 4:6085-90.

[23] Vilarrasa V, Bolster D, Dentz M, Carrera J. Semianalytical solution for CO_2 plume shape and pressure evolution during CO_2 injection in deep saline formations. Transp. Porous Media 2013; 97:43-65.

[24] Birkholzer JT, Zhou Q, Tsang C-F. Large-scale impact of CO_2 storage in deep saline aquifers: A sensitivity study on pressure response in stratified systems. Int. J. Greenh. Gas Control 2009; 3:181–94.

[25] Zhang Z, Agarwal RK. Numerical simulation and optimization of CO_2 sequestration in saline aquifers for vertical and horizontal well injection. Comput. Geosci. 2012; 16:891–99.

[26] Okwen RT, Stewart MT, Cunningham JA. Temporal variations in near-wellbore pressures during CO_2 injection in saline aquifers. Int. J. Greenh. Gas Control 2011; 5:1140–48.

[27] Rutqvist J, Tsang C-F. A study of caprock hydromechanical changes with CO_2 injection into a brine formation. Environ. Geol. 2002; 42:296–305.

[28] Streit JE, Hillis RR. Estimating fault stability and sustainable fluid pressures for underground storage of CO_2 in porous rock. Energy 2004; 29:1445-56.

[29] Vilarrasa V, Carrera J, Olivella S. Hydromechanical characterization of CO_2 injection sites. Int. J. Greenh. Gas Control 2013; doi:10.1016/j.ijggc.2012.11.014.

[30] Bennion B, Bachu S. Drainage and imbibition relative permeability relationships for supercritical CO_2/brine and H_2S/brine systems in intergranular sandstone, carbonate, shale, and anhydrite rocks. SPE Reservoir Evaluation & Eng. 2008; 11:487-96.

[31] van Genuchten R. A closed-form equation for predicting the hydraulic conductivity of unsaturated soils. Soil Sci. Soc. Am. J. 1980; 44:892–98.

[32] Zienkiewicz OC, Cormeau IC. Visco-plasticity – plasticity and creep in elastic solids – a unified numerical solution approach. Int. J. Numer. Methods Eng. 1974; 8:821–45.

[33] Jaeger JC, Cook NGW, Zimmerman RW. Fundamentals of rock mechanics. 4th Edition, Wiley-Blackwell, Oxford; 2007.

[34] Olivella S, Carrera J, Gens A, Alonso EE. Non-isothermal multiphase flow of brine and gas through saline media. Transp. Porous Media 1994; 15:271–93.

[35] Olivella S, Gens A, Carrera J, Alonso EE. Numerical formulation for a simulator (CODE_BRIGHT) for the coupled analysis of saline media. Eng. Computations 1996; 13:87–112.

[36] de Simone S, Vilarrasa V, Carrera J, Alcolea A, Meier P. Thermal coupling may control mechanical stability of geothermal reservoirs during cold water injection. Physics and Chemistry of the Earth 2013; doi:10.1016/j.pce.2013.01.001.

[37] Hsieh PA. Deformation-induced changes in hydraulic head during ground-water withdrawal. Ground Water 1996; 34(6):1082–89.

[38] Vilarrasa V, Silva O, Carrera J, Olivella S. Liquid CO_2 injection for geological storage in deep saline aquifers. Int. J. Greenh. Gas Control 2013; 14:84–96.

[39] Barton N, Bandis S, Bakhtar K. Strength, deformation and conductivity coupling of rock joints. Int. J. Rock Mech. Min. Sci. Geomech. Abstracts 1985; 22 (3):121–40.

[40] Yeo IW, De Freitas MH, Zimmerman RW. Effect of shear displacement on the aperture and permeability of rock. Int. J. Rock Mech. Min. Sci. 1998; 35(8):1051–70.

[41] Vilarrasa V, Koyama T, Neretnieks I, Jing L. Shear-induced flow channels in a single rock fracture and their effect on solute transport. Transp. Porous Media 2011; 87(2):503–23.

[42] Neuzil CE. Groundwater flow in low-permeability environments. Water Res. Res. 1986; 22(8):1163–95.

[43] Denney D. Continuous improvement led to the longest horizontal well. J. Petroleum Technology 2009; 61:55-56.

[44] Okwen RT, Stewart MT, Cunningham JA. Effect of well orientation (vertical vs horizontal) and well length on the injection of CO_2 in deep saline aquifers. Transp. Porous Media 2011; 90:219–32.

[45] Korbol R, Kaddour A. Sleipner vest CO_2 disposal - injection of removed CO_2 into the Utsira formation. Energy Convers. Mgmt. 1995; 36 (6-9):509–12.

[46] Rutqvist J, Vasco DW, Myer L. Coupled reservoir-geomechanical analysis of CO_2 injection and ground deformations at In Salah, Algeria. Int. J. Greenh. Gas Control 2010; 4:225–30.

[47] Rinaldi AP, Rutqvist J. Modeling of deep fracture zone opening and transient ground surface uplift at KB-502 CO_2 injection well, In Salah, Algeria. Int. J. Greenh. Gas Control 2013; 12:155–67.

[48] Preisig M, Prévost JH. Coupled multi-phasse thermo-poromechanical effects. Case study: CO_2 injection at In Salah, Algeria. Int. J. Greenh. Gas Control 2011; 5(4):1055–64.

[49] Bissell RC, Vasco DW, Atbi M, Hamdani M, Okwelegbe M,Goldwater MH. A full field simulation of the In Salah gas production and CO_2 storage project using a coupled geo-mechanical and thermal fluid Flow simulator. Energy Procedia 2011; 4:3290–97.

[50] Paterson L, Ennis-King J, Sharma S. Observations of thermal and pressure transients in carbon dioxide wells. In: Proceedings of the SPE annual technical conference and exhibition. Florence, Italy; 19-22 September 2010.

TABLES

Table 1. Properties of the rocks considered in the model

Property	Saline aquifer	Caprock	Upper aquifer	Basal aquifer
Young's modulus, E (GPa)	10	5	2.5	20
Poisson ratio, ν (-)	0.3	0.3	0.3	0.3
Porosity, ϕ (-)	0.1	0.01	0.1	0.1
Intrinsic permeability, k (m^2)	10^{-13}	10^{-18}	10^{-14}	10^{-14}
Relative liquid permeability, k_{rl} (-)	S_l^3	S_l^6	S_l^3	S_l^3
Relative gas permeability, k_{rg} (-)	S_g^3	S_g^6	S_g^3	S_g^3
Gas entry pressure, P_0 (MPa)	0.02	1.0	0.02	0.02
Van Genuchten shape parameter, m (-)	0.8	0.3	0.8	0.8

Table 2. Maximum mobilized friction angle for a CO_2 injection of 20 years. The value on the left of the slash is for a NF stress regime and the one on the right of the slash corresponds to a RF stress regime.

	Vertical well		Horizontal well	
	Saline aquifer [a]	Caprock [b]	Saline aquifer [a]	Caprock [b]
Base case	22.2/21.7	19.9/21.1	19.8/34.6	19.8/32.9
Higher k_{cap}	21.5/21.2	20.5/21.0	20.8/22.2	20.3/22.3
Lower E_{aq}	21.9/21.3	20.2/20.9	19.8/32.5	19.8/29.6
Higher Q_m	24.3/23.8	19.9/22.5	19.9/59.6	19.8/58.5
Longer L			21.2/22.9	19.8/21.5

[a] The mobilized friction angle is measured at the top of the saline aquifer next to the injection well casing.

[b] The mobilized friction angle is measured at a point placed 5 m above the saline aquifer next to the injection well casing.

FIGURES

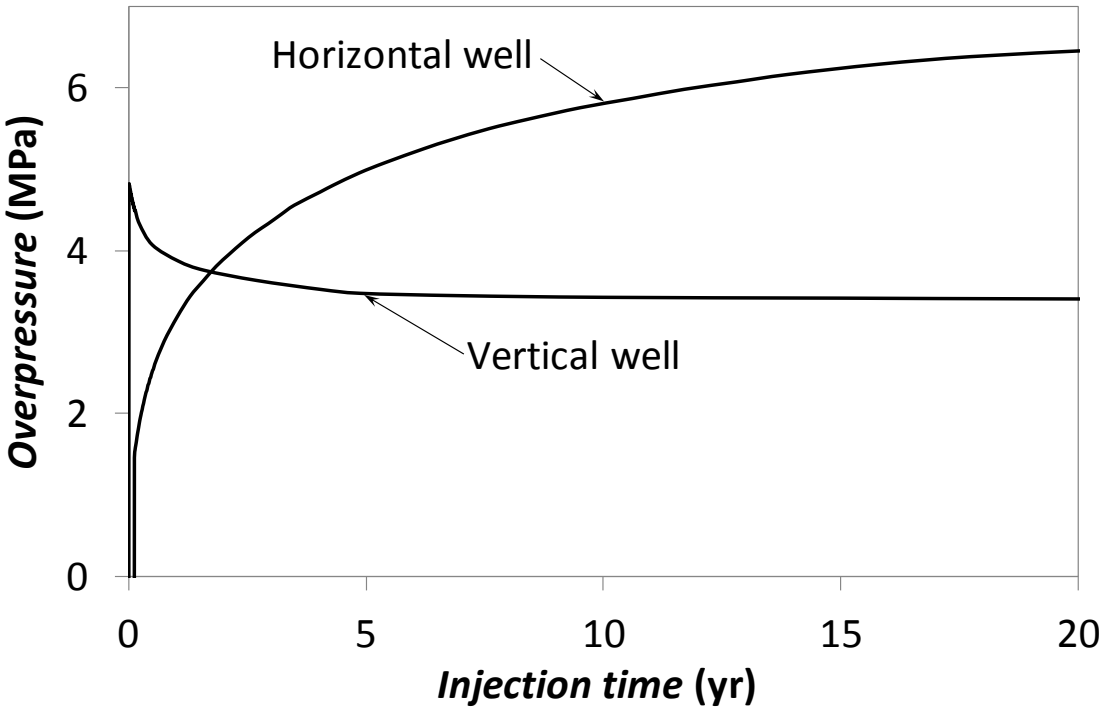

Figure 1. Overpressure evolution at the top of the aquifer next to the injection well casing when injecting CO_2 through a vertical and a horizontal well at a constant mass flow rate.

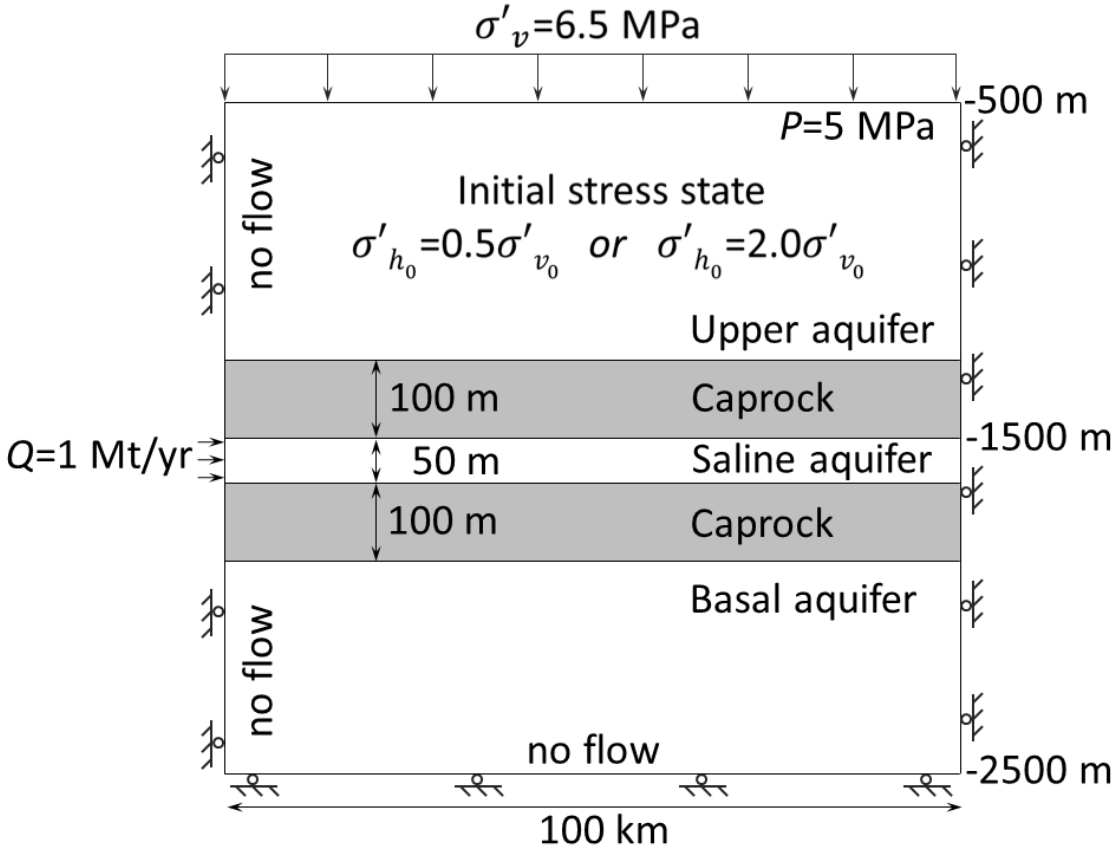

Figure 2. Schematic description of the hydro-mechanical model and boundary conditions. CO_2 is uniformly injected along the whole thickness of the saline aquifer in the vertical well (using an axisymmetric model), while it is injected at the bottom of the saline aquifer in the horizontal well (modeling half of a vertical cross section perpendicular to the horizontal well).

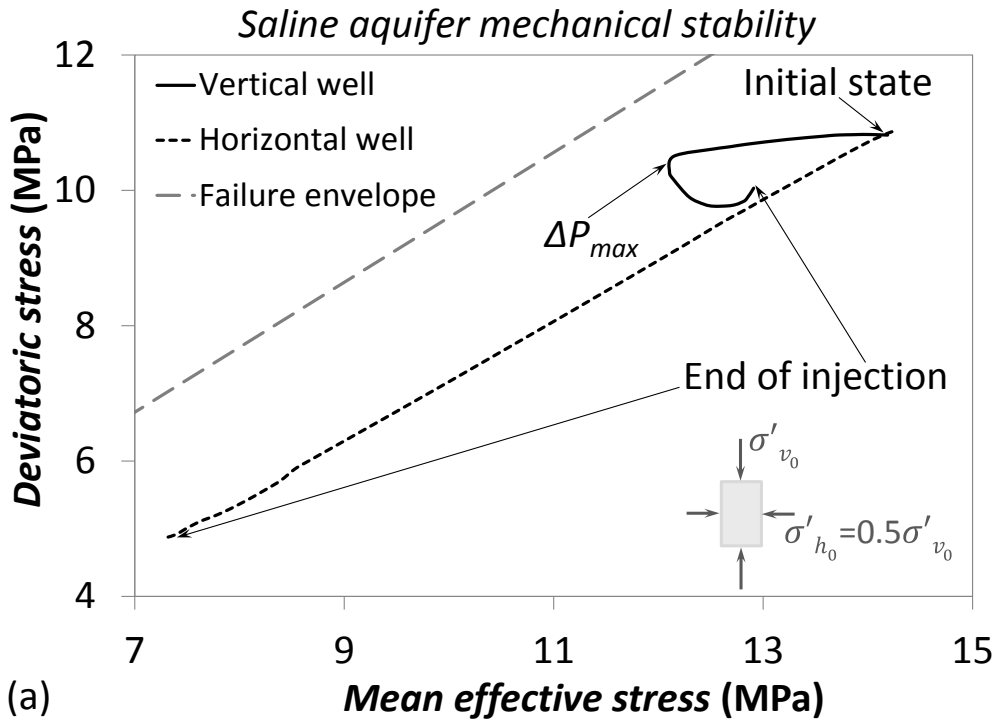

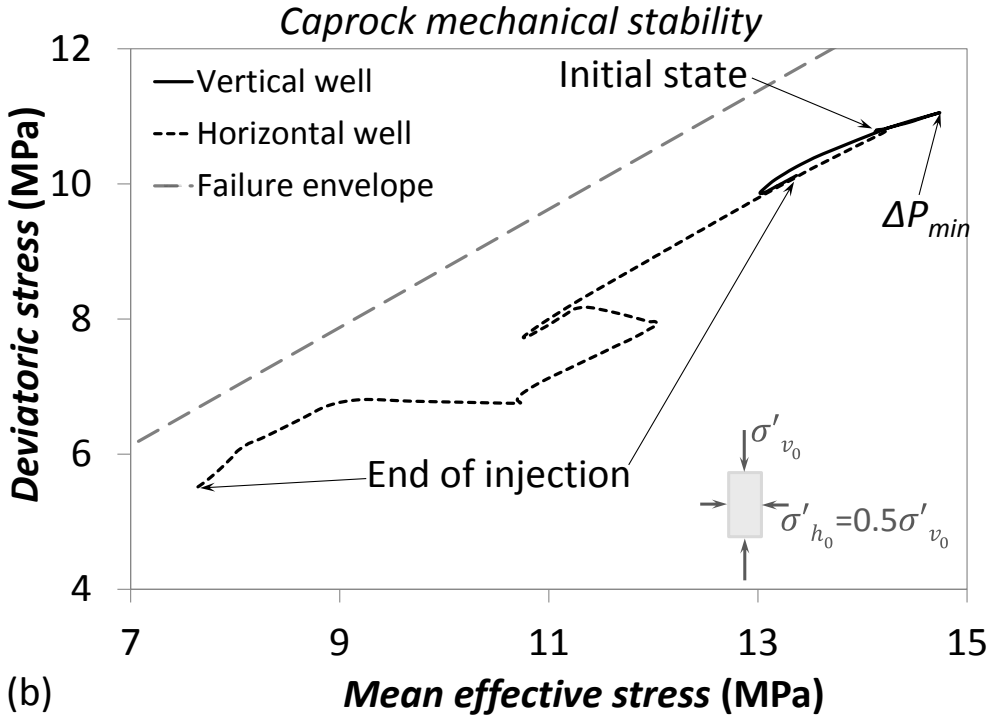

Figure 3. $q-\sigma'_m$ trajectories for a vertical and a horizontal well in a normal faulting stress regime (a) at the top of the saline aquifer next to the injection well casing and (b) at a point of the caprock placed 5 m above the saline aquifer next to the injection well casing.

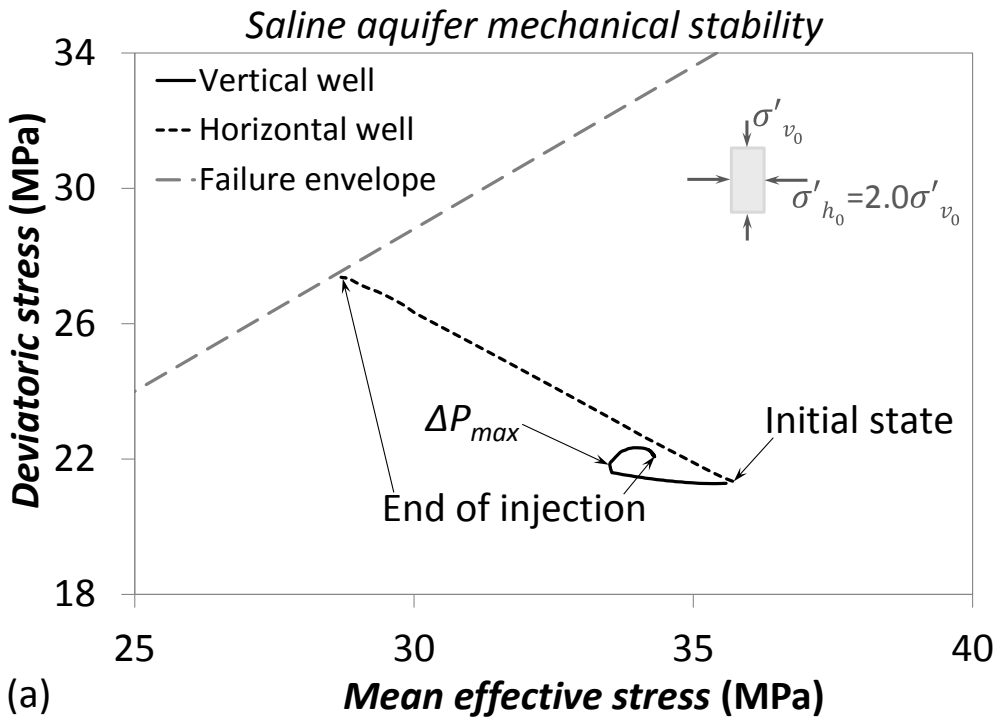

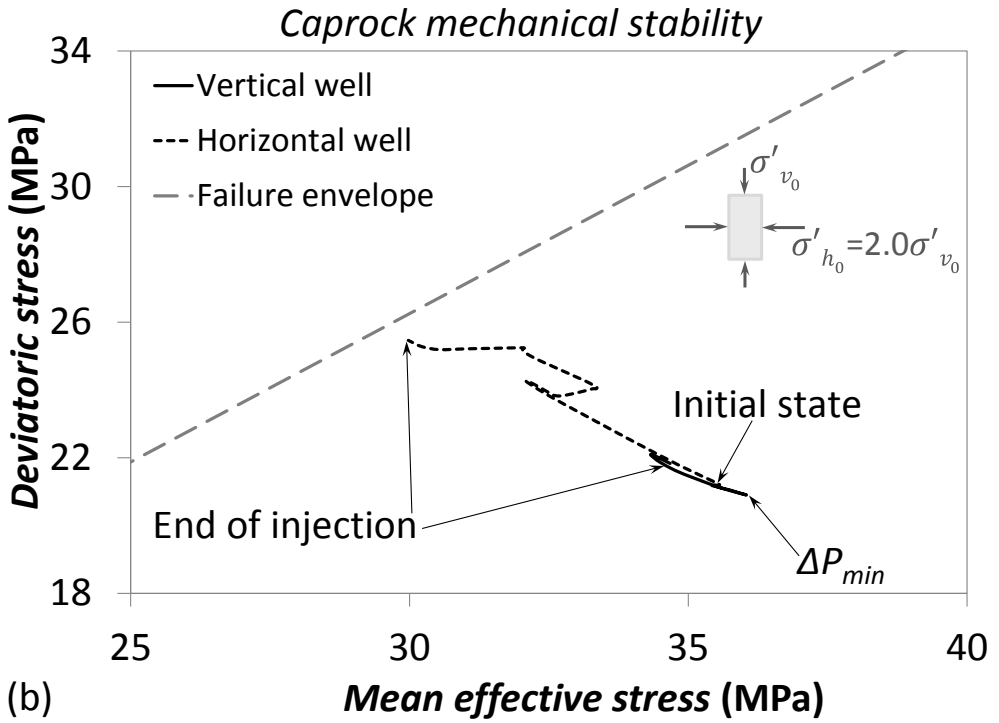

Figure 4. $q-\sigma'_m$ trajectories for a vertical and a horizontal well in a reverse faulting stress regime (a) at the top of the saline aquifer next to the injection well casing and (b) at a point of the caprock placed 5 m above the saline aquifer next to the injection well casing.

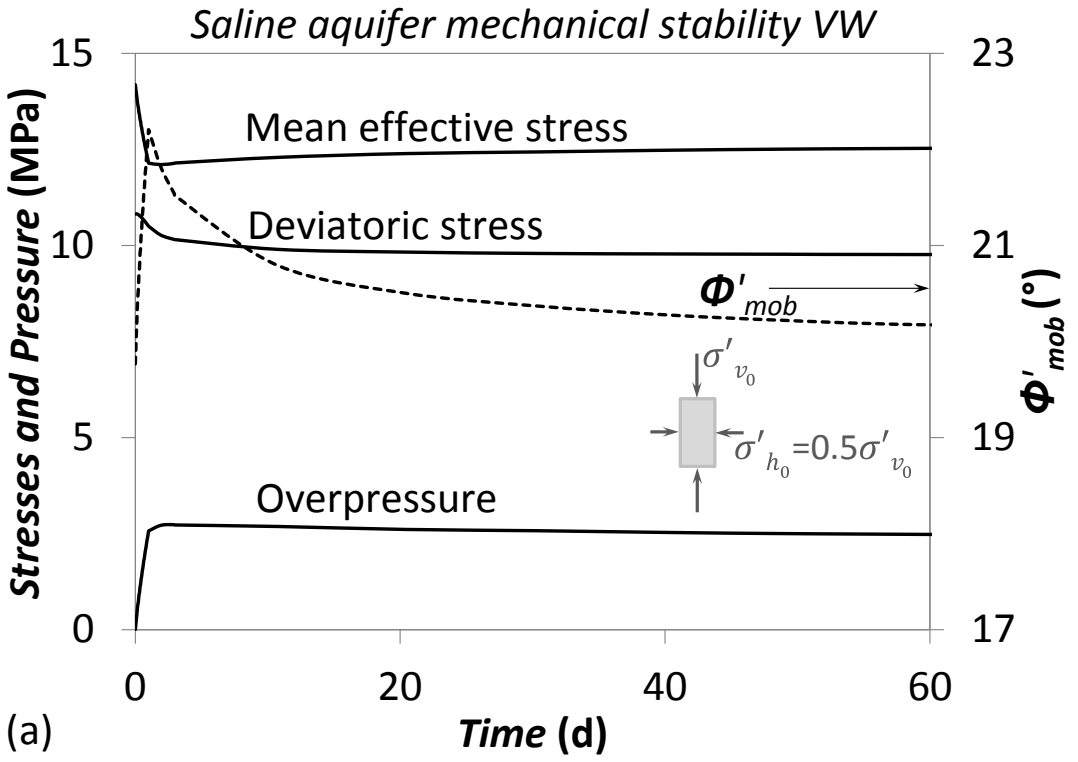

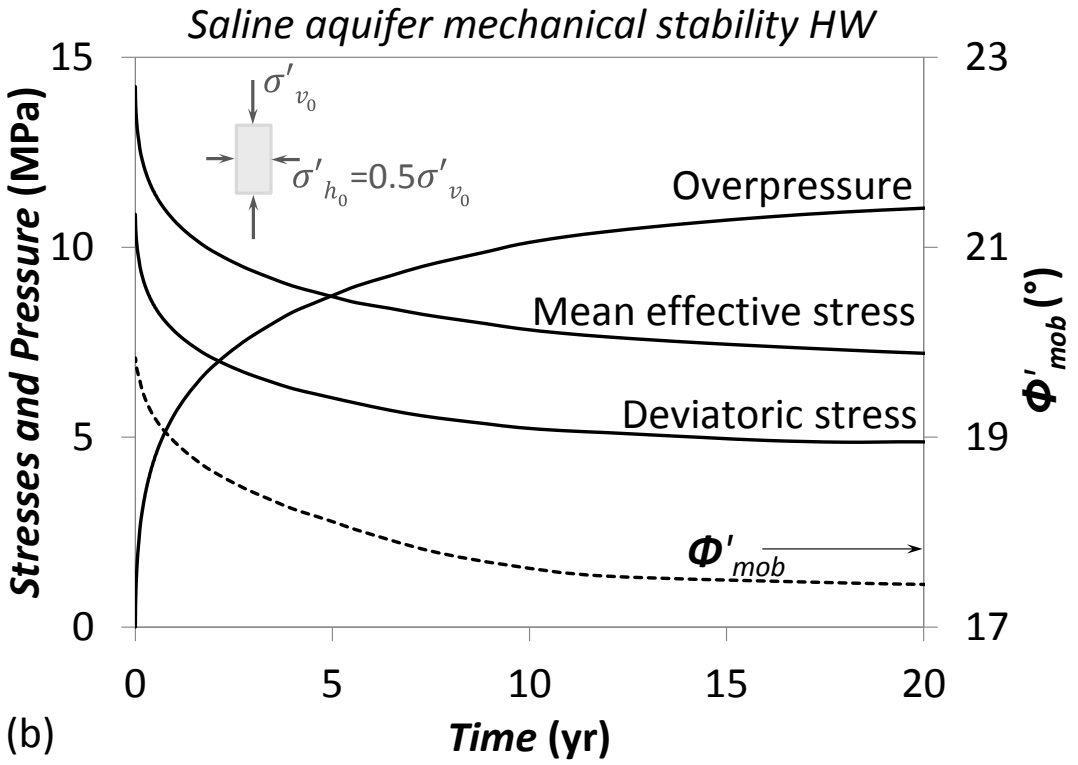

Figure 5. Stress, overpressure and mobilized friction angle evolution in a normal faulting stress regime at the top of the saline aquifer next to the injection well casing (a) for a vertical well (VW) and (b) for a horizontal well (HW).

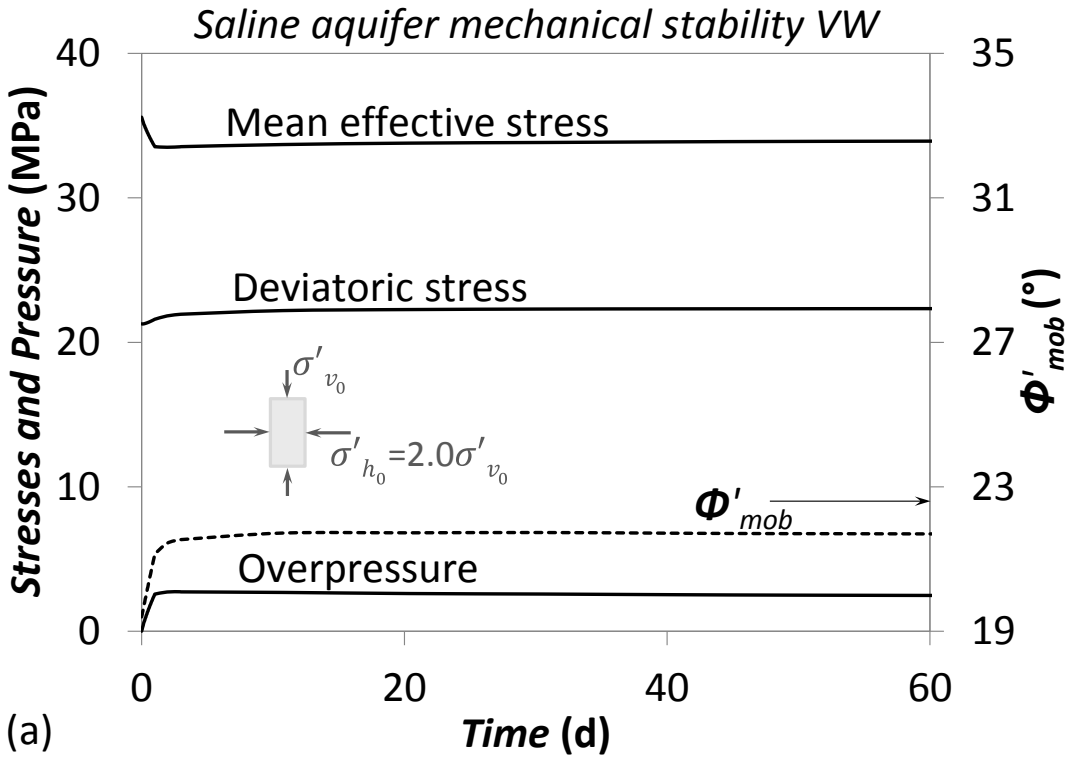

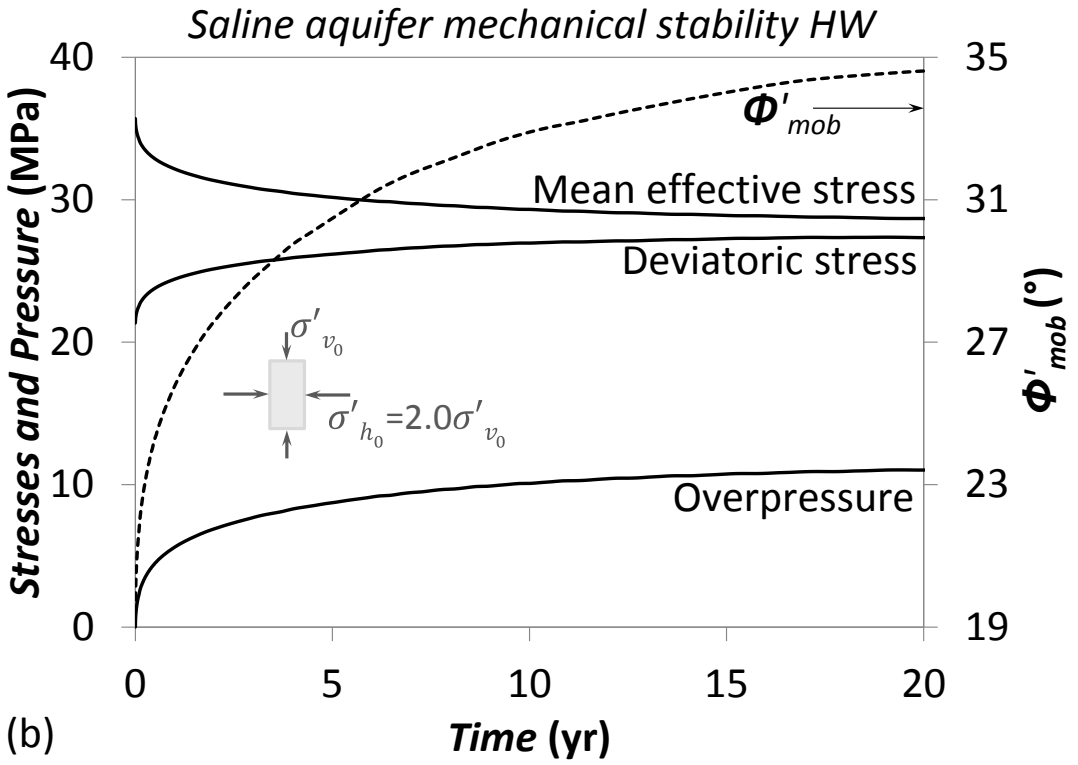

Figure 6. Stress, overpressure and mobilized friction angle evolution in a reverse faulting stress regime at the top of the saline aquifer next to the injection well casing (a) for a vertical well (VW) and (b) for a horizontal well (HW).

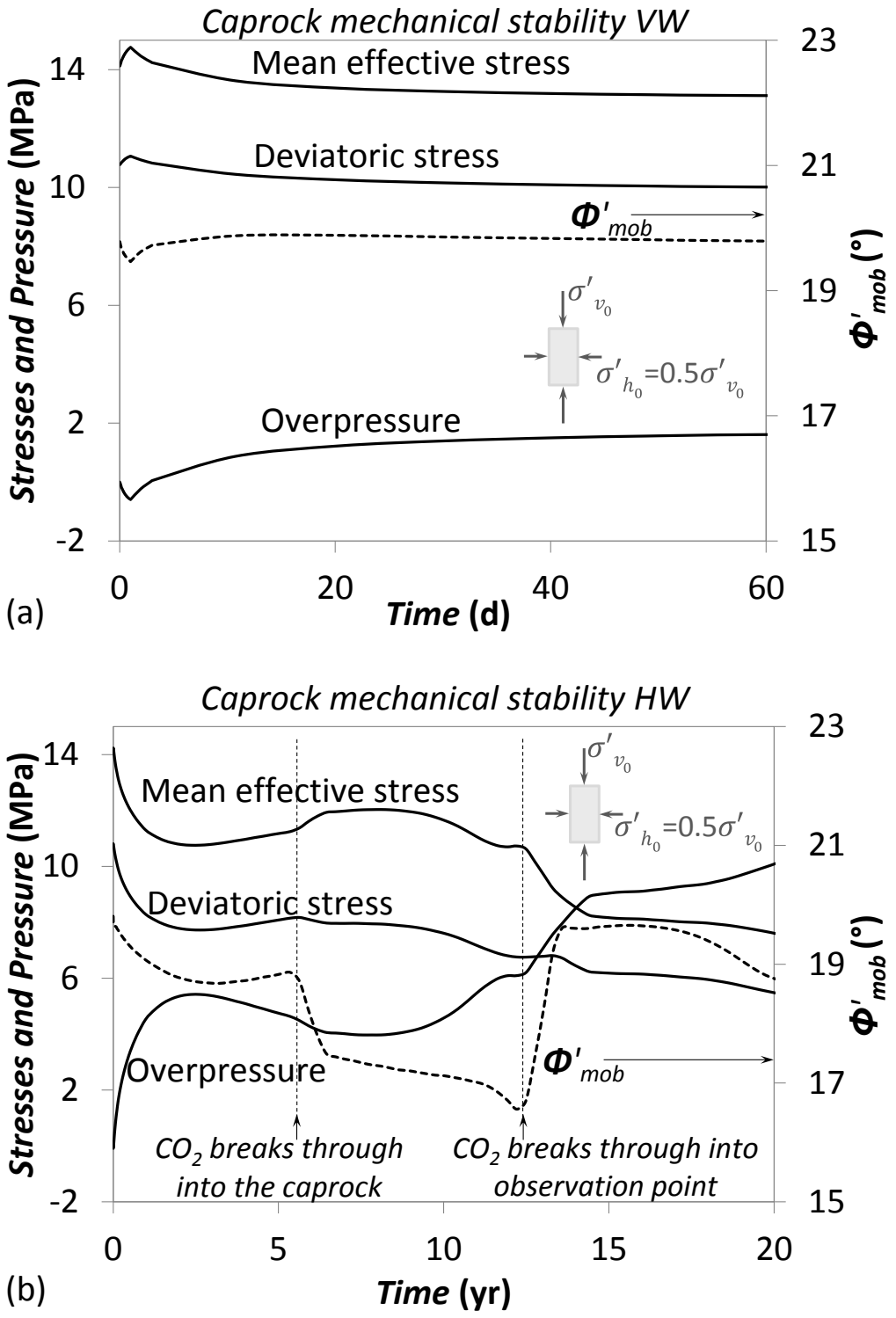

Figure 7. Stress, overpressure and mobilized friction angle evolution in a normal faulting stress regime at a point of the caprock placed 5 m above the saline aquifer next to the injection well casing (a) for a vertical well (VW) and (b) for a horizontal well (HW).

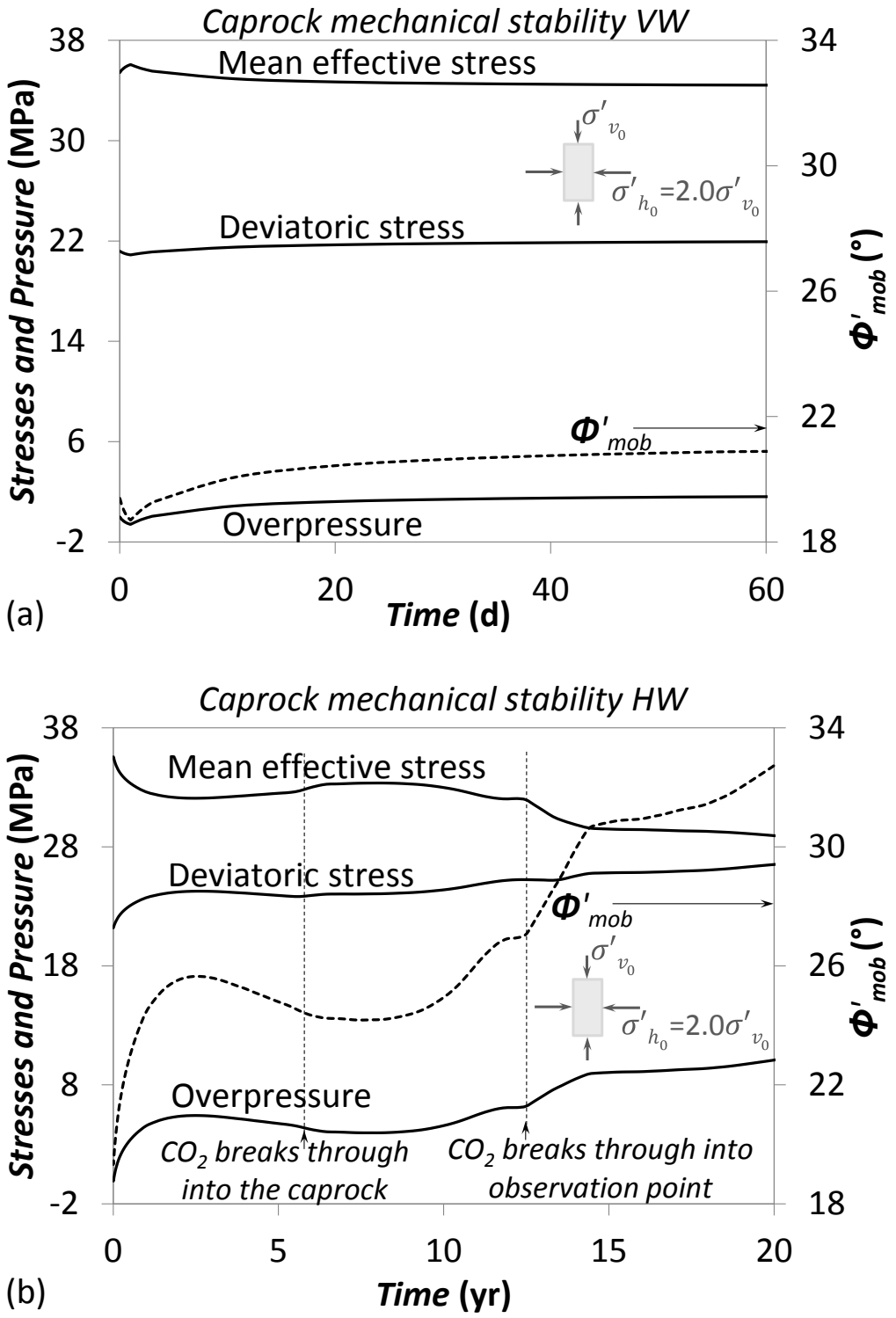

Figure 8. Stress, overpressure and mobilized friction angle evolution in a reverse faulting stress regime at a point of the caprock placed 5 m above the saline aquifer next to the injection well casing (a) for a vertical well (VW) and (b) for a horizontal well (HW).

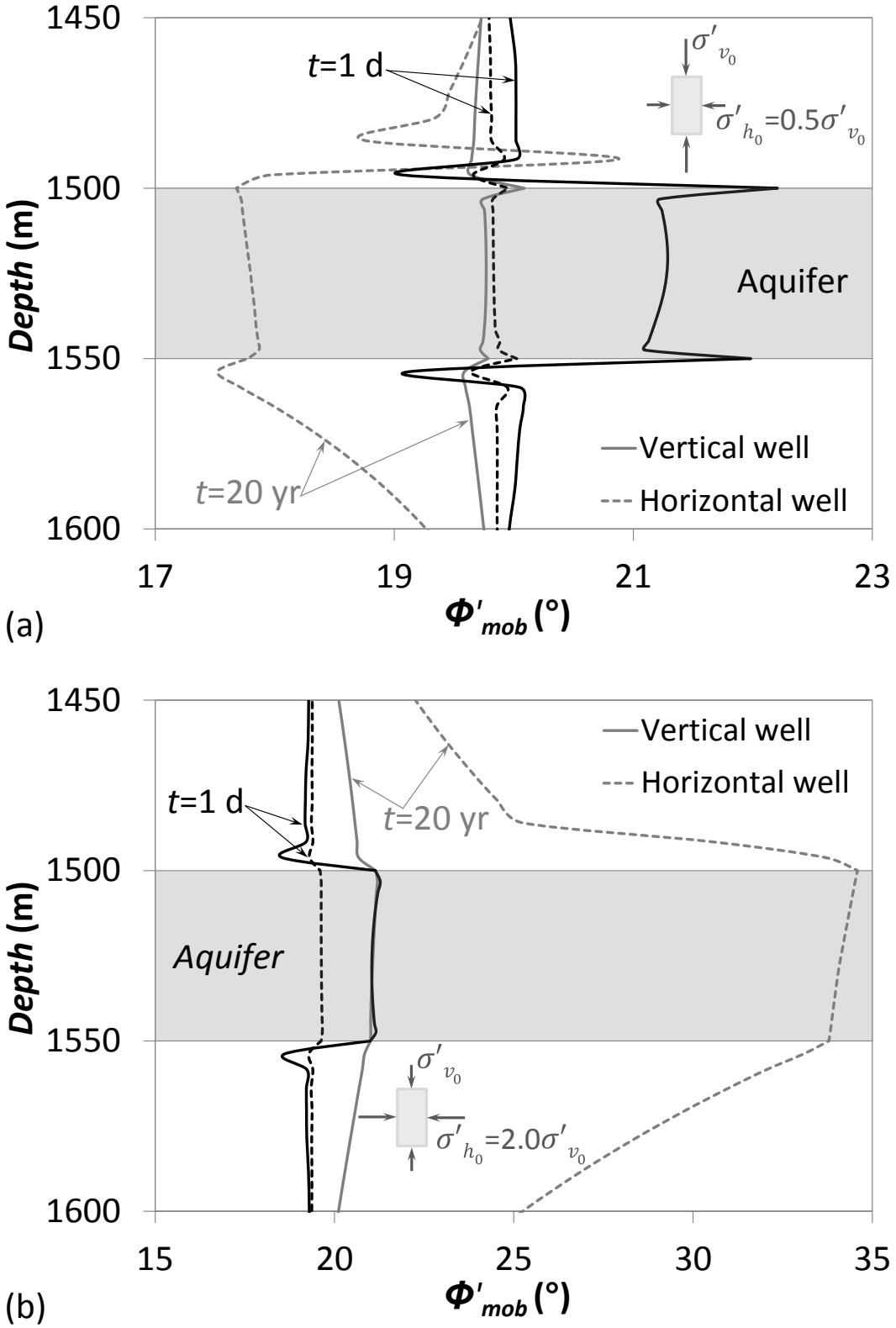

Figure 9. Mobilized friction angle for a vertical and a horizontal well in a vertical cross section that is tangent to the well casing after 1 day and 20 years of injecting 1 Mt/yr of CO_2 in (a) a normal faulting stress regime and (b) a reverse faulting stress regime.

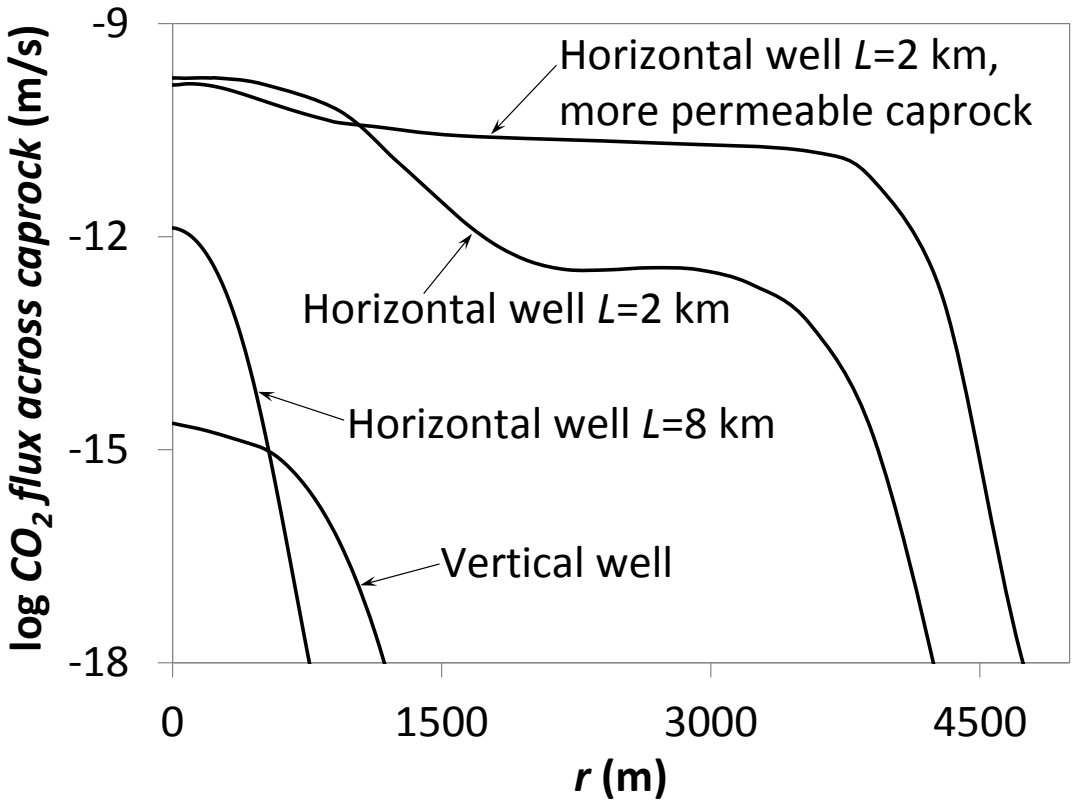

Figure 10. Vertical CO_2 across a horizontal section of the caprock placed 5 m above the saline aquifer after 20 years of injecting 1 Mt/yr for several scenarios.